Neuronal interaural level difference response shifts are level-dependent in the rat auditory cortex

Michael Kyweriga, Whitney Stewart and Michael Wehr

J Neurophysiol 111:930-938, 2014. First published 11 December 2013; doi:10.1152/jn.00648.2013

J Neurophysiol 111: 930–938, 2014.
First published December 11, 2013; doi:10.1152/jn.00648.2013.

Neuronal interaural level difference response shifts are level-dependent in the rat auditory cortex

Michael Kyweriga,[1,2] Whitney Stewart,[1,3] and Michael Wehr[1,4]

[1]*Institute of Neuroscience, University of Oregon, Eugene, Oregon;* [2]*Department of Biology, University of Oregon, Eugene, Oregon;* [3]*Department of Human Physiology, University of Oregon, Eugene, Oregon; and* [4]*Department of Psychology, University of Oregon, Eugene, Oregon*

Submitted 10 September 2013; accepted in final form 8 December 2013

Kyweriga M, Stewart W, Wehr M. Neuronal interaural level difference response shifts are level-dependent in the rat auditory cortex. *J Neurophysiol* 111: 930–938, 2014. First published December 11, 2013; doi:10.1152/jn.00648.2013.—How does the brain accomplish sound localization with invariance to total sound level? Sensitivity to interaural level differences (ILDs) is first computed at the lateral superior olive (LSO) and is observed at multiple levels of the auditory pathway, including the central nucleus of inferior colliculus (ICC) and auditory cortex. In LSO, this ILD sensitivity is level-dependent, such that ILD response functions shift toward the ipsilateral (excitatory) ear with increasing sound level. Thus early in the processing pathway changes in firing rate could indicate changes in sound location, sound level, or both. In ICC, while ILD responses can shift toward either ear in individual neurons, there is no net ILD response shift at the population level. In behavioral studies of human sound localization acuity, ILD sensitivity is invariant to increasing sound levels. Level-invariant sound localization would suggest transformation in level sensitivity between LSO and perception of sound sources. Whether this transformation is completed at the level of the ICC or continued at higher levels remains unclear. It also remains unknown whether perceptual sound localization is level-invariant in rats, as it is in humans. We asked whether ILD sensitivity is level-invariant in rat auditory cortex. We performed single-unit and whole cell recordings in rat auditory cortex under ketamine anesthesia and measured responses to white noise bursts presented through sealed earphones at a range of ILDs. Surprisingly, we found that with increasing sound levels ILD responses shifted toward the ipsilateral ear (which is typically inhibitory), regardless of whether cells preferred ipsilateral, contralateral, or binaural stimuli. Voltage-clamp recordings suggest that synaptic inhibition does not contribute substantially to this transformation in level sensitivity. We conclude that the level invariance of ILD sensitivity seen in behavioral studies is not present in rat auditory cortex.

auditory cortex; interaural level difference; level dependence; sound localization

DETERMINING THE LOCATION of unseen predators, prey, and conspecifics is one of the primary functions of the auditory system. Mammals use three cues to localize sounds: interaural time differences (ITDs), interaural level differences (ILDs), and the head-related transfer function (for review, see Grothe et al. 2010). In animals that hear primarily in the high-frequency range, such as the rat (Heffner et al. 1994; Kelly and Masterton 1977), ILD is the primary cue used to determine sound locations on the horizontal azimuth (Kapfer et al. 2002; Wesolek et al. 2010). ILD sensitivity is first computed in the lateral superior olive (LSO) (Kavanagh and Kelly 1992; Moore and Caspary 1983). In the LSO, neuronal ILD response shifts are strongly level-dependent (Tsai et al. 2010). This means that early in the processing pathway changes in firing rate could indicate changes in sound location, sound level, or both. Yet in psychometric behavioral tasks, ILD sensitivity does not shift with increasing sound levels in macaques (Recanzone and Beckerman 2004) or humans (Altshuler and Comalli 1975; Sabin et al. 2005). How, then, does the brain accomplish sound localization with invariance to total sound level? ILD sensitivity is also observed in higher structures such as the central nucleus of inferior colliculus (ICC) (Irvine and Gago 1990; Pollak et al. 1986; Semple and Kitzes 1987) and the auditory cortex (Kelly and Sally 1988; Phillips and Irvine 1983; Zhang et al. 2004). In the LSO, increasing ipsilateral sound levels cause spiking response functions in the LSO to shift toward the ipsilateral ear (Tsai et al. 2010). In the ICC, approximately half of the cells are invariant to increasing sound levels and the remaining cells have leftward, rightward, or mixed shifts with no net shift at the population level (Park et al. 2004). Taken together, these results suggest a gradual transformation from strong level dependence in the LSO to level invariance in the perception of sound source location. Consistent with this, a few free-field studies have shown level invariance of azimuth tuning in the auditory cortex of cats (Mickey and Middlebrooks 2003), bats (Razak 2011), and primates (Zhou and Wang 2012), but level dependence of ILD coding in the auditory cortex has not been tested.

Rodents, especially the rat and mouse, are increasingly important model organisms in auditory neuroscience. The rodent auditory system is similar in many ways to those of cats and primates but different in other ways (for review, see Phillips et al. 2012). For example, ITD and ILD processing differs markedly between rats and other species, such as the cat and primate, which have larger heads (Heffner 2004; Wesolek et al. 2010). It is unknown whether ILD sensitivity in the rat auditory cortex depends on sound level or is level-invariant. It is also unknown whether rats show perceptual invariance to increasing sound levels. On the basis of previous work in the auditory cortex of cats, bats, and primates, we predicted that ILD response functions in the rat auditory cortex would also be level-invariant. To test this hypothesis, we measured ILD response functions of rat auditory cortical neurons at different sound levels. Surprisingly, we found that ILD responses strongly shifted toward the ipsilateral ear with increasing sound levels in both spiking output and subthreshold membrane potential responses. To understand how this transformation is accomplished, we used in vivo whole cell recordings to mea-

Address for reprint requests and other correspondence: M. Wehr, 1254 Univ. of Oregon, Eugene OR, 97403-1254 (e-mail: wehr@uoregon.edu).

sure ILD response functions for synaptic excitation and inhibition. The results suggest that these shifts are not created in the cortex by synaptic processing and are instead consistent with inheritance from presynaptic neurons. We conclude that level invariance of ILD sensitivity is not present in the rat auditory cortex.

METHODS

All procedures were in strict accordance with National Institutes of Health guidelines and were approved by the University of Oregon Institutional Animal Care and Use Committee.

Physiology. We recorded from the left auditory cortex of 86 anesthetized (30 mg/kg ketamine, 0.24 mg/kg medetomidine) albino rats (*Rattus norvegicus*, Sprague Dawley), aged 19–28 (mean = 23.4, SD = 2.7) postnatal days. We used this age range to improve the yield of in vivo whole cell recordings (Scholl et al. 2010). Rats older than 14–19 days, like adults, orient correctly toward sounds on the horizontal plane (Kelly et al. 1987). The critical period for hearing in rats is complete by approximately postnatal day 14 (de Villers-Sidani et al. 2007), although some limited additional maturation of receptive fields and synaptic markers (e.g., NR1, GluR2, and GAD65) occurs until approximately postnatal day 28 (Chang et al. 2005; Lu et al. 2008; Popescu and Polley 2010; Xu et al. 2007, 2010). We tested whether any of our neural ILD measures depended on age within this range (see below for details of these measures and how they were computed). We found no significant effect of age on ILD shifts based on integrated membrane potential ($R^2 = 0.029$, $P = 0.06$), firing rate ($R^2 = 0.003$, $P = 0.62$), inhibitory conductance (G_I; $R^2 = 0.004$, $P = 0.65$), or excitatory conductance (G_E; $R^2 = 0.003$, $P = 0.71$), indicating that these measures are developmentally stable (and likely mature) during this age range. Nevertheless, it is important to note that our results do not rule out possible changes in cortical ILD processing in adulthood (i.e., >28 days).

At the beginning of each experiment we used tungsten microelectrodes (1–2 MΩ, FHC) to coarsely map the auditory cortex, using multiunit recordings. We sought to locate sites with robust binaural response properties. Approximately 80% of neurons in this report were located in either the primary auditory cortex (A1) or suprarhinal auditory field (SRAF) (Higgins et al. 2010; Polley et al. 2007), with the remainder from either ventral (VAF) or posterior (PAF) auditory field. We identified A1 from the caudal-rostral tonotopic gradient. We also targeted SRAF, which contains a relatively high proportion of cells preferring central ILDs (Higgins et al. 2010). We identified SRAF from the absence of auditory evoked responses along its ventral border.

Single-unit recordings. We obtained single-unit recordings with the loose cell-attached patch method, which provides excellent single-unit isolation. We only included cells in our sample if they had at least one spike following stimulus onset (0–125 ms; $n = 117$ cells) and a minimum of five trials per stimulus combination. Subpial depth for these cells ranged from 111 to 1,015 μm (mean = 573.8 μm, SD = 205.3), as determined from micromanipulator travel.

Whole cell recordings. We used standard blind patch-clamp methods to obtain 166 whole cell recordings. We only included cells in our sample if they had stable prestimulus resting membrane potentials (−50 to 0 ms) that were within 5 mV between the beginning and end of the recording. Subpial depth for these cells ranged from 122 to 844 μm (mean = 389.6 μm, SD = 146.3). We did not use voltage-gated channel blockers in the pipette solution, so that we could record both spiking output and synaptic currents from the same cells. The internal solution contained (in mM), 120 K-gluconate, 2 $MgCl_2$, 0.05 $CaCl_2$, 4 MgATP, 0.4 NaGTP, 10 Na_2 phosphocreatine, 10 HEPES, and 13 BAPTA, pH 7.28, diluted to 297 mosM, producing a calculated inhibitory reversal potential of −91.1 mV and an excitatory reversal potential of 3.4 mV. We corrected for a calculated liquid junction potential of 15.0 mV (Barry 1994), based on standard extracellular ionic concentrations (Sykova 1997), body temperature of 37°C, and dilution of our internal solution concentrations by ~10% (to achieve physiological osmolarity).

In a subset of cells we also obtained voltage-clamp recordings. Holding potentials were stepped (with a 1-s ramp) to a pseudorandom sequence of two values with an Axopatch 200B amplifier. At each potential, after a 1-s equilibration period, ten 10-mV voltage pulses were delivered to monitor series and input resistance, followed by acoustic stimuli. For our sample of neurons recorded with voltage clamp, input resistance was 55.6 ± 30.2 MΩ and series resistance was 48.3 ± 4.2 MΩ (median ± interquartile range, $n = 73$ cells). We measured synaptic currents at two holding potentials (mean = −108.2 mV, SD = 4.7 and mean = +27.5 mV, SD = 19.5; corrected for series resistance and liquid junction potential) and for 5–10 trials (median 10) for each acoustic stimulus. Synaptic conductances, corrected for series resistance, were computed off-line assuming an isopotential neuron (for details, see Wehr and Zador 2003). To ensure high-quality voltage-clamp recordings, we discarded cells that failed to show evoked conductances > 0.5 nS and a minimum of five trials for each stimulus combination, resulting in a sample of 73 neurons.

In summary, we recorded from 117 cells with the loose cell-attached method and 166 cells with the whole cell current-clamp method. Our whole cell data set contained 78 spiking cells recorded in current-clamp mode, which were added to the cell-attached data set to create a total of 195 spiking cells. Our whole cell data set also contained 73 cells recorded in voltage-clamp mode.

Sound stimuli. All stimuli were generated with custom software in MATLAB (MathWorks, Natick, MA) at a sampling rate of 192 kHz with a Lynx-TWO-B sound card and delivered with Etymotics ER-2 earphones in sealed ear configuration. These earphones were suitable for our experiments as the rat audiogram is 7 octaves (0.5–64 kHz; Heffner et al. 1994; Kelly and Masterton 1977) and the ER-2 earphones cover over half of this range (4 octaves: 1–16 kHz). All experiments were performed in a double-walled sound isolation chamber with anechoic surface treatment. We sealed the Etymotics ER-2 earphones along with Knowles omnidirectional electret condenser microphones into each ear.

The sound level inside each ear canal was calibrated with the Knowles microphones, which were in turn calibrated with a Bruel & Kjaer 4939 1/4-in. microphone prior to each experiment. To characterize binaural response properties we used pseudorandomly interleaved white noise bursts (25-ms duration) presented simultaneously to each ear from 10 to 50 decibel (dB) sound pressure level, in 10-dB steps (noise was not frozen between left and right or between each level). This produced an array of 25 binaural stimuli, with a range of average binaural levels (ABLs; defined as the average of the levels presented to the 2 ears) from 10 to 50 dB, across a range of ILDs from −40 to +40 dB (corresponding to the maximum physiological range of ILD; Koka et al. 2008). Figure 1*B* shows this stimulus array with both coordinate systems included; ILD is on the *x*-axis and ABL is on the *y*-axis, whereas the levels in the ipsilateral ear and contralateral ear are on the diagonal axes (rotated by 45°). We restricted sound levels to a maximum of 50 dB because we noted that higher levels produced cross talk from one ear to the other, presumably due to sound transmission through the head (data not shown). We defined contralateral ILDs as positive. All stimuli had 5-ms onset and offset ramps with 500-ms interstimulus intervals.

For whole cell recordings, we first recorded membrane potential responses to our stimulus set in current-clamp mode. Then we switched to voltage-clamp mode and measured the synaptic currents evoked by the same stimuli. Because of time constraints, we were only able to measure the characteristic frequency (CF) in a subset of our recorded cells ($n = 47$ cells). We presented a monaural tuning curve to the contralateral ear comprised of pure tones, at five intensities from 10 to 50 dB and at four frequencies per octave from 1 to 16 kHz. As with our binaural stimulus set, all tuning curve stimuli

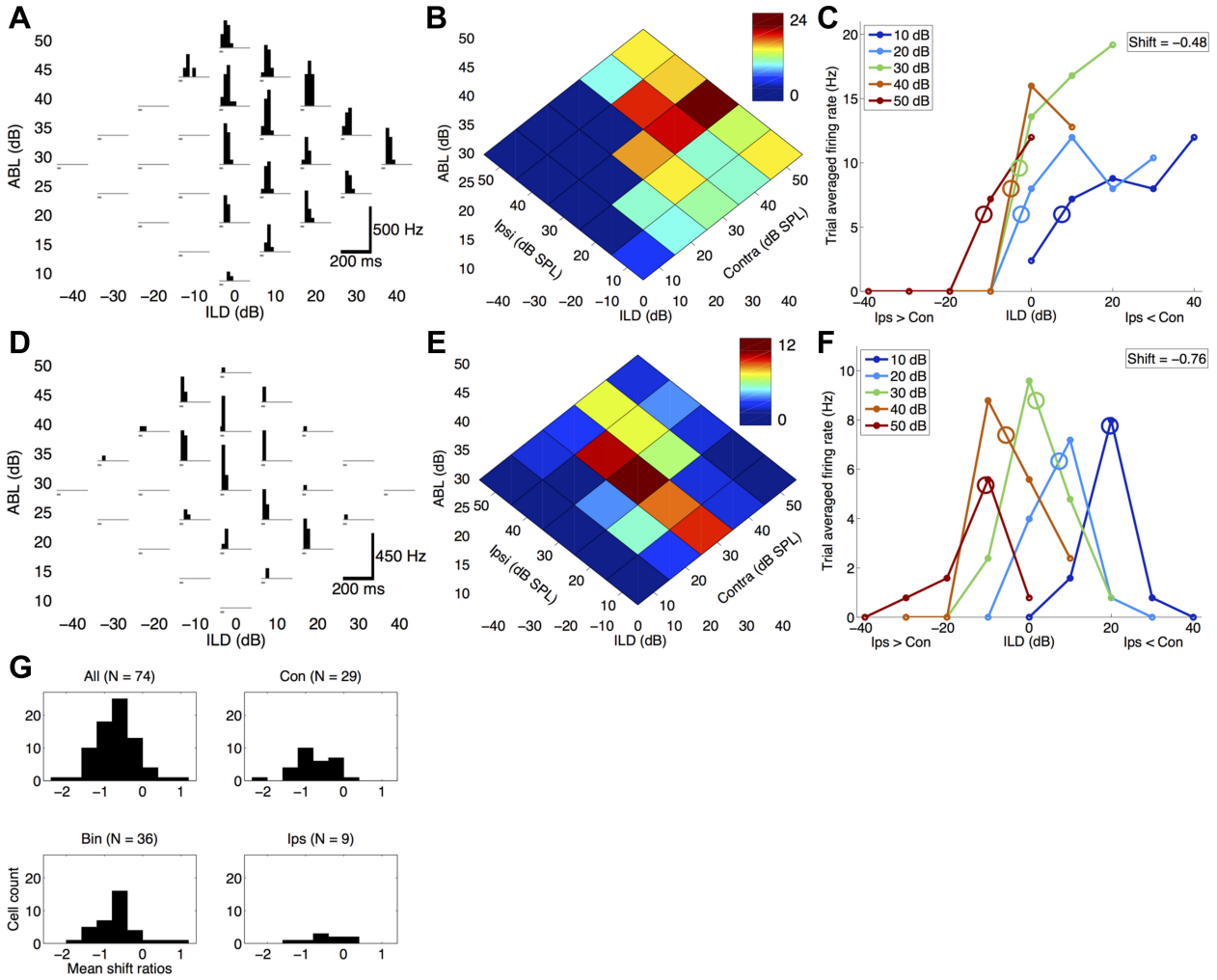

Fig. 1. Spiking interaural level difference (ILD) responses in the rat auditory cortex shift toward the ipsilateral ear (negative shifts) with increasing ipsilateral sound level. *A–F*: 2 representative examples showing negative ILD response shifts in both contralateral-preferring (*A–C*; *cell 120810-MK-3-2*) and binaural-preferring (*D–F*; *cell 091410-WS-2-1*) cells. *A* and *D*: spiking responses to the binaural stimulus array. Each histogram shows the firing rate in 20-ms bins (accumulated from 10 trials). White noise bursts (25-ms duration) are indicated in gray. *B* and *E*: trial-averaged normalized firing rate heat maps of the same data shown in *A* and *D*. Dark red indicates maximum firing rate, and dark blue indicates minimum firing rate. Each binaural stimulus can be represented either as an ILD-average binaural level (ABL) combination (*x*- and *y*-axes) or as a contralateral and ipsilateral sound level (diagonal axes). For example, the green response at ILD 20, ABL 20 corresponds to Contra 30, Ipsi 10. *C* and *F*: firing rate ILD response curves. Ipsilateral level is held constant for each curve (see *inset* for color code) as a function of ILD. In other words, each line is a diagonal slice through *B*, parallel to the Contra axis. *C*: contralateral-preferring cell with a mean ILD response shift of −0.48 dB/dB (SD = 0.44; see METHODS for detailed description). Circles denote half-maximal ILD values. Negative ILDs correspond to greater ipsilateral level (Ips > Con); positive ILDs correspond to greater contralateral level (Ips < Con). *F*: binaural-preferring cell with a mean ILD response shift of −0.76 dB/dB (SD = 0.33). Circles denote the average of left and right half-maximal ILD values; thus the circles are found near the maxima. *G*: population histograms showing that the majority of cells (89.2%) have negative response shifts (*top left*, 66/74 cells), regardless of binaural preference categorization (Con, contralateral preferring; Bin, binaural preferring; Ips, ipsilateral preferring).

were 25 ms with 5-ms onset and offset ramps and were presented with 500-ms interstimulus intervals. We determined the CF by finding the frequency eliciting the greatest response at the lowest intensity (for details, see Polley et al. 2007).

Data analysis. To extract spikes, we first high-pass filtered extracellular and intracellular recorded voltages at 300 Hz (Butterworth filter) and used an absolute threshold of 1–5 mV (median = 5 mV; mean = 3.7 mV, SD = 1.8). We quantified spiking responses by counting spikes in a 125-ms window beginning at sound stimulus onset in 20-ms bins (Fig. 1, *A* and *D*). Baseline firing rate, computed in the 375-ms window ending at sound onset (i.e., the remainder of the interstimulus interval), was subtracted from each spiking response (note that baseline firing rate in Fig. 1, *C* and *F*, is zero). We then set negative firing rates to zero.

We quantified membrane potential responses by integrating the trial-averaged membrane potential in the 200-ms window following stimulus onset wherever the membrane potential was significantly above baseline (z score with $P < 0.05$; red region in Fig. 2, *A* and *D*). Similarly, we quantified synaptic conductance responses by integrating conductances in the 200-ms window following sound onset wherever the conductance was significantly above zero ($P < 0.05$). We set negative conductances to zero.

ILD response shift calculation. We calculated ILD response shifts for each cell (Park et al. 2004; Tsai et al. 2010). In our binaural stimulus set, for each ipsilateral level, we presented the rat with five contralateral levels from 10 to 50 dB (in 10-dB steps), thereby creating a stimulus array of five ILDs for each ipsilateral sound level. Since these response functions could be monotonic or nonmonotonic, we employed two different methods to determine the ILD response shift.

The first method focused on responses that increased or decreased monotonically with ILD (i.e., for contralateral-preferring or ipsilater-

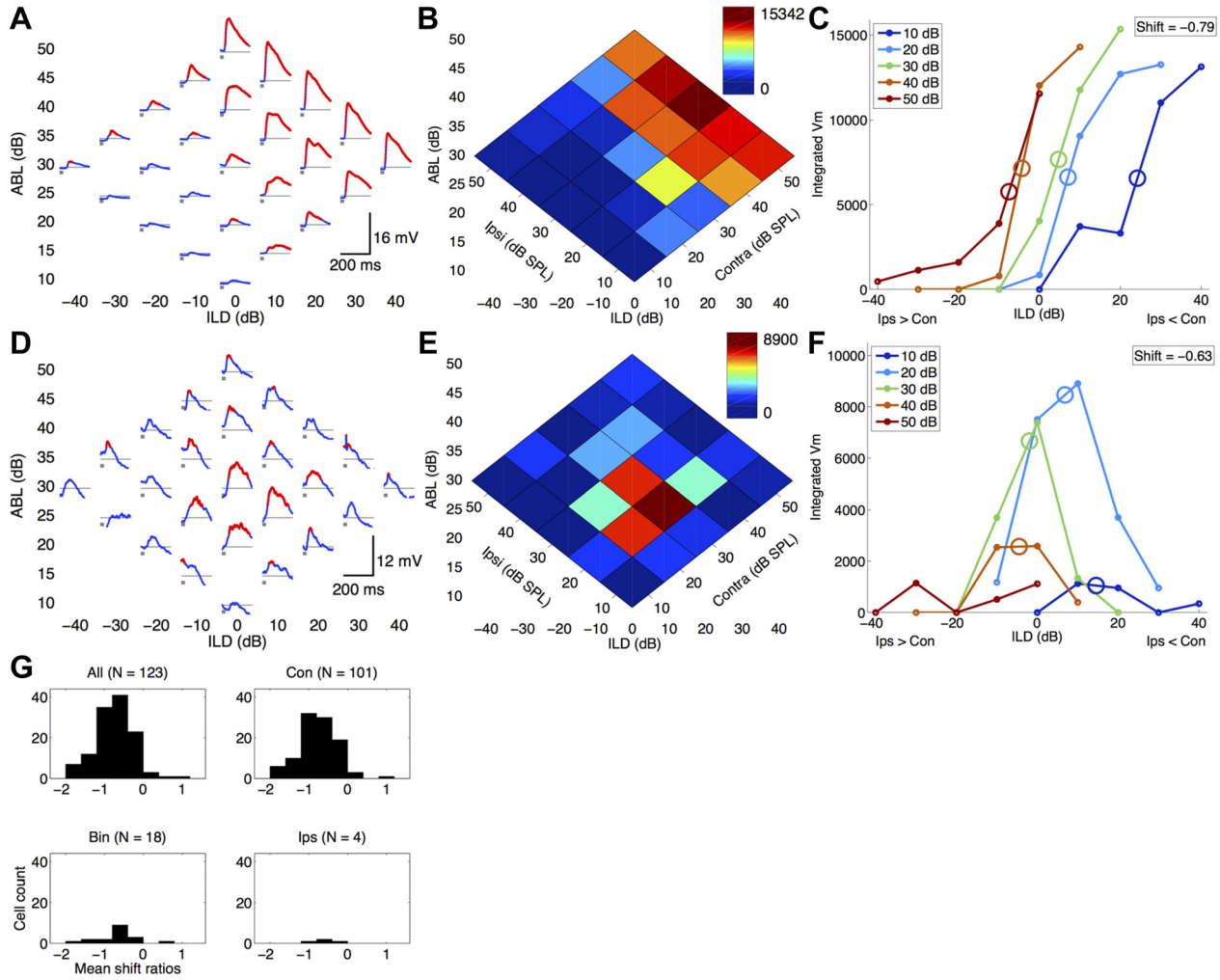

Fig. 2. Membrane potential (V_m) ILD responses in the rat auditory cortex shift toward the ipsilateral ear with increasing ipsilateral sound level. *A–F*: 2 representative examples showing negative ILD response shifts in both contralateral-preferring (*A–C*; *cell 010511-MK-3-8*) and binaural-preferring (*D–F*; *cell 080910-MK-2-2*) nonspiking cells. *A* and *D*: membrane potential responses to the binaural stimulus array. Each subplot shows the membrane potential (*A*: mean of 20 trials; *D*: mean of 10 trials). White noise bursts (25 ms duration) are indicated in gray. Resting membrane potential (V_{rest}) is indicated by horizontal thin gray line (*A*: $V_{rest} = -78.8$ mV; *D*: $V_{rest} = -60.2$ mV). Red regions are significantly above baseline and were included in the integrated membrane potential responses in *B* and *C*. *B* and *E*: normalized integrated membrane potential heat maps of the same data shown in *A* and *D*. Dark red indicates maximum depolarization, and dark blue indicates minimum depolarization. *C* and *F*: integrated membrane potential ILD response curves. Ipsilateral level held constant for each curve as a function of ILD. *C*: contralateral-preferring cell with a mean ILD response shift of −0.79 dB/dB (SD = 0.68). *F*: binaural-preferring cell with a mean ILD response shift of −0.63 dB/dB (SD = 0.33). *G*: population histograms showing that the majority of cells (95.9%) have negative membrane potential response shifts (*top left*, 118/123 cells), regardless of binaural preference categorization.

al-preferring cells, respectively). To determine the ILD response shift, we first sought a reliable point on each ILD response function that could be used to measure shifts. For this we chose the half-maximal ILD, which is at the steepest part of the ILD response function and is therefore the most reliable point for measuring shifts. To find the half-maximal ILD, we first measured the maximum of the trial-averaged ILD response function. To ensure that these peak responses were significant, for spiking responses we only included ILD response functions where the peak ILD response was >1 SD above the baseline firing rate; for membrane potential and conductance responses, we only integrated responses when they were significantly above baseline. We then found the half-maximal response value (halfway between the maximum value and the prestimulus baseline). The half-maximal ILD was defined as the interpolated ILD that produced the half-maximal response value for each ipsilateral stimulus array. These half-maximal values are indicated by circles in Fig. 1*C*.

We then measured the mean ILD response shift for a cell as the average difference between the half-maximal ILDs for the ILD response functions at each ipsilateral sound level, divided by the change in ipsilateral sound level. For example, in Fig. 1*C*, the dark blue (7.5 dB) and light blue (−2.5 dB) circles are separated by 10 dB, producing a leftward ILD response shift of −10 dB (−2.5 minus 7.5 dB) caused by a 10-dB increase in ipsilateral sound level. This response shift is therefore −10/10 = −1 dB/dB. Altogether, Fig. 1*C* has four half-maximal ILD shifts of −10 (−2.5 minus 7.5 dB), −0.4 (−2.9 minus −2.5 dB), −2.1 (−5 minus −2.9 dB), and −6.7 (−11.7 minus −5 dB) dB, each caused by 10-dB increases in ipsilateral sound levels. This produced four respective response shifts of −1, −0.04, −0.21, and −0.67 dB/dB with a mean response shift of −0.48 dB/dB (SD = 0.44). Thus, on average, for each decibel increase in sound level, the ILD response function of this cell shifted 0.48 dB toward the ipsilateral ear. Note that if we instead calculate the total ILD response shift [e.g., (−11.7 − 7.5)/(50 − 10) = −0.48], we obtain the same result and our overall results remain unchanged (data not shown), as others have reported (Park et al. 2004; Tsai et al. 2010). Negative response shifts indicate leftward shifts toward the ipsilateral ear, and positive response shifts indicate rightward shifts toward the contralateral ear. Response shifts of zero indicate invariance with respect to increasing sound levels.

The second method for calculating response shifts focused on responses that were nonmonotonic as a function of ILD (i.e., for binaural-preferring cells), for which we slightly modified the first method. For each ipsilateral stimulus array, we measured the half-maximal response values falling on either side of the peak response of firing rate (Fig. 1*F*), integrated membrane potential (Fig. 2*F*), or integrated conductances (data not shown). We then took the average of these two half-maximal ILD values, resulting in a single value approximately corresponding to the peak of the ILD response function (Fig. 1*F* and Fig. 2*F*, circles). We then used this point to compute the ILD response shifts as described above for contralateral and ipsilateral cells.

For both methods, in order to calculate the response shift, at least two half-maximal ILDs in a single binaural category were required; otherwise the cell was discarded. For example, some response functions had multiple half-maximal values or were unresponsive. Thus for these response functions it was not possible to determine half-maximal ILDs, and these response functions were omitted from our analysis (e.g., Fig. 2*F*, red trace). We also tested a more rigorous criterion requiring each cell to produce at least three half-maximal ILDs. While this reduced our sample size by ~50% for spiking, membrane potential, and conductance measures, our results remained unchanged (data not shown). We did not compute response shifts between half-maximal values computed by two different methods within a cell. For example, no shift was calculated for ILD response functions that were monotonic at one ipsilateral sound level and nonmonotonic at another.

To test the significance of the response shifts computed for each cell, we used bootstrap resampling to produce a distribution of 100 resampled response shifts for spiking, membrane potential, and conductance data. We then tested whether these distributions were significantly less than zero, using the one-sample *t*-test for each cell.

RESULTS

Spiking ILD responses in rat auditory cortex shift toward ipsilateral ear with increasing ipsilateral sound level. We obtained spiking output from 195 cells, using both the loose cell-attached method (117 cells) and the whole cell method (78 cells in current-clamp mode). Representative examples of two cells are shown in Fig. 1, *A–F*. Figure 1, *A–C*, show an example of a contralateral-preferring cell, often referred to in the literature as binaurally inhibited (EI or EO/I; Razak and Fuzessery 2010; Zhang et al. 2004). This cell type shows robust firing to contralateral (+10 to +40 ILDs) and some central (−10 to +10 ILDs) sounds but did not respond to ipsilateral stimuli (−40 to −10 ILDs; Fig. 1, *A* and *B*). Figure 1*C* shows that the ILD response curves shifted −19.2 dB (−11.7 − 7.5 dB; Fig. 1*C*, red and dark blue circles, respectively; see METHODS) when ipsilateral levels were increased from 10 to 50 dB. This corresponded to a −0.48 dB/dB average response shift for this cell (SD = 0.44). In other words, for each 1-dB increase in ipsilateral level, the ILD response functions shifted 0.48 dB toward the ipsilateral ear. This response shift was highly significant (P = 1.41e-43, as determined by bootstrap resampling, mean shift: −0.51, SD = 0.21; see METHODS).

Figure 1, *D–F*, show an example of a binaural-preferring cell, also referred to in the literature as binaurally facilitated (PB or EE/F; Zhang et al. 2004), predominantly binaural (PB; Razak and Fuzessery 2010), or peaked (Razak 2011). This cell type shows robust firing to central sounds (−10 to +10 ILDs) but weak or no responses to either contralateral (+10 to +40 ILDs) or ipsilateral (−40 to −10 ILDs) sounds (Fig. 1, *D* and *E*). Figure 1*F* shows that the ILD response curves shifted −30.3 dB (−10.6 − 19.7 dB; Fig. 1*F*, red and dark blue circles, respectively), when ipsilateral levels increased from 10 to 50 dB. This corresponded to a −0.76 dB/dB response shift for this cell (SD = 0.33). This response shift was highly significant (P = 6.72e-122, mean bootstrapped shift: −0.77, SD = 0.05).

In our sample of spiking cells, 74/195 had robust ILD response functions and met our inclusion criteria (see METHODS). Of these cells, 66/74 had negative response shifts, with a mean shift of −0.69 dB/dB (SD = 0.54). This population average shift was significantly negative (P = 3.8e-17, 1-sample *t*-test), and each of the 66/74 negative response shifts was significantly negative (at the $P < 0.05$ level, as tested by bootstrap resampling). Previous studies have used an arbitrary criterion of −0.4 dB/dB to classify response shifts as significant (Park et al. 2004; Tsai et al. 2010); by this measure, 55/74 of our cells (74.3%) were significantly below this criterion (P = 1.6e-5, 1-sample *t*-test). There were no significant differences between the response shifts in each binaural preference category (independent samples *t*-test, all $P > 0.25$). We conclude that the spiking responses of auditory cortical neurons overwhelmingly show negative ILD response shifts with increasing sound level.

In a subset of our spiking data set (47/195 cells), we measured the CF of the cell by presenting a frequency-intensity tuning curve to the contralateral ear. We then presented the rat with the binaural stimulus array at the cell's CF (47 cells: 40 cell attached, 7 whole cell). From this sample, 16/47 cells had robust ILD responses and met our inclusion criteria. Consistent with our much larger white noise sample, 15/16 cells had negative response shifts, with a mean shift of −0.85 dB/dB (SD = 0.6). This population average shift was significantly negative (P = 4.59e-5, 1-sample *t*-test), and each of the 15/16 negative response shifts was significantly negative (at the $P < 0.05$ level, as tested by bootstrap resampling). We found that 75% of our cells had response shifts that were significantly lower than the arbitrary criterion of −0.4 dB/dB (12/16 cells, P = 8.9e-3, 1-sample *t*-test). This result indicates that leftward ILD response shifts are not specific to white noise stimuli and are a more general property of the rat auditory cortex.

Membrane potential ILD responses in rat auditory cortex shift toward ipsilateral ear with increasing ipsilateral sound level. About half of the neurons in our whole cell sample (88/166) did not fire any spikes in response to our binaural stimuli. This is consistent with previous reports of sparse spiking responses in the auditory cortex (Chadderton et al. 2009; DeWeese et al. 2003; Hromadka et al. 2008). In fact, this proportion is probably an underestimate of the prevalence of nonspiking cells, since we often aborted recordings from nonspiking cells. However, we wondered whether ILD response shifts also occurred for subthreshold membrane potential responses. Representative examples of two nonspiking cells are shown in Fig. 2, *A–F*. Figure 2, *A–C*, show an example of a nonspiking contralateral-preferring cell. This cell showed membrane potential depolarizations to contralateral (+10 to +40 ILDs) and some central (−10 to +10 ILDs) sounds but had only very weak responses to ipsilateral stimuli (−40 to −10 ILDs; Fig. 2, *A* and *B*). To calculate the ILD response functions for each ipsilateral level, we integrated the average membrane potential depolarization wherever it was signifi-

cantly above baseline (z score $P < 0.05$, red regions in Fig. 2, *A* and *D*) for each stimulus combination. Increasing ipsilateral sound levels from 10 to 50 dB caused the ILD response curve to shift −31.7 dB (−7.5 − 24.2 dB; Fig. 2*C*, red and dark blue circles, respectively), with an average response shift of −0.79 dB/dB (SD = 0.68). This response shift was highly significant (P = 1.7e-117, mean bootstrapped shift: −0.80, SD = 0.06).

Figure 2, *D–F*, show an example of a nonspiking binaural-preferring cell. This cell responded to central (−10 to +10 ILDs) sounds but had weak or no responses to either contralateral (+10 to +40 ILDs) or ipsilateral (−40 to −10 ILDs) sounds (Fig. 2, *D* and *E*). Figure 2*F* shows that increasing ipsilateral levels from 10 to 40 dB caused the ILD response curves to shift −19 dB (−4.5 − 14.5; Fig. 2*F*, orange and dark blue circles, respectively). This corresponded to a mean response shift of −0.63 dB/dB (SD = 0.33). This response shift was highly significant (P = 1.41e-43, as determined by bootstrap resampling, mean shift: −0.75, SD = 0.32; see METHODS).

In our whole cell sample, 123/166 had robust ILD responses and met our inclusion criteria. Of these cells, we found that 118/123 had negative response shifts, with a mean shift of −0.74 dB/dB (SD = 0.48), which was significantly negative at the population level (P = 1.06e-33, 1-sample t-test). Each of the 118/123 negative response shifts was significantly negative (at the $P < 0.05$ level, as tested by bootstrap resampling). We found no significant differences between the response shifts in each binaural preference category (independent samples t-test, all $P > 0.54$). Again, using an arbitrary cutoff of −0.4 dB/dB, we found that 77.2% of our cells had response shifts that were significantly lower than this cutoff value (95/123 cells, P = 3.49e-12, 1-sample t-test). We conclude that, like spiking responses, subthreshold membrane potential responses also show negative ILD response shifts with increasing sound level.

Both excitatory and inhibitory responses in rat auditory cortex shift toward ipsilateral ear with increasing ipsilateral sound level. Within our sample of whole cell recordings we were also able to obtain voltage-clamp recordings in 73/166 cells. Only cells that responded with peak responses of at least 0.5 nS and had at least five trials per stimulus combination were included in this count. Figure 3, *A–C*, show a representative example of excitatory and inhibitory inputs in a contralateral-preferring cell. This cell showed G_Es to contralateral (+10 to +40 ILDs) and central (−10 to +10 ILDs) sounds but not to ipsilateral stimuli (−40 to −10 ILDs; Fig. 3*A*, green shows G_E). While G_Is were observed at all ILDs (Fig. 3*A*, red shows G_I), note the reduction in G_I magnitude when comparing ipsilateral ILDs to central and contralateral ILDs. To calculate the ILD response functions for each ipsilateral level, we separately integrated the G_E (Fig. 3*B*) and G_I (Fig. 3*C*) at all sample points when the synaptic conductance was significantly above zero ($P < 0.05$). Increasing ipsilateral sound levels from 10 to 50 dB caused the integrated G_Es to shift −26.8 dB (−12.7 − 14.1; Fig. 3*B*, red and dark blue circles, respectively), with an average response shift of −0.67 dB/dB (SD = 0.61). This response shift was highly significant (P = 2.0e-153, mean bootstrapped shift: −0.67, SD = 0.02). Increasing ipsilateral sound levels from 10 to 50 dB caused the integrated G_Is to shift −29.5 dB (−18.6 − 10.9; Fig. 3*C*, orange and dark blue circles, respectively), with an average response shift of −0.98 dB/dB (SD = 0.4). This response shift was highly

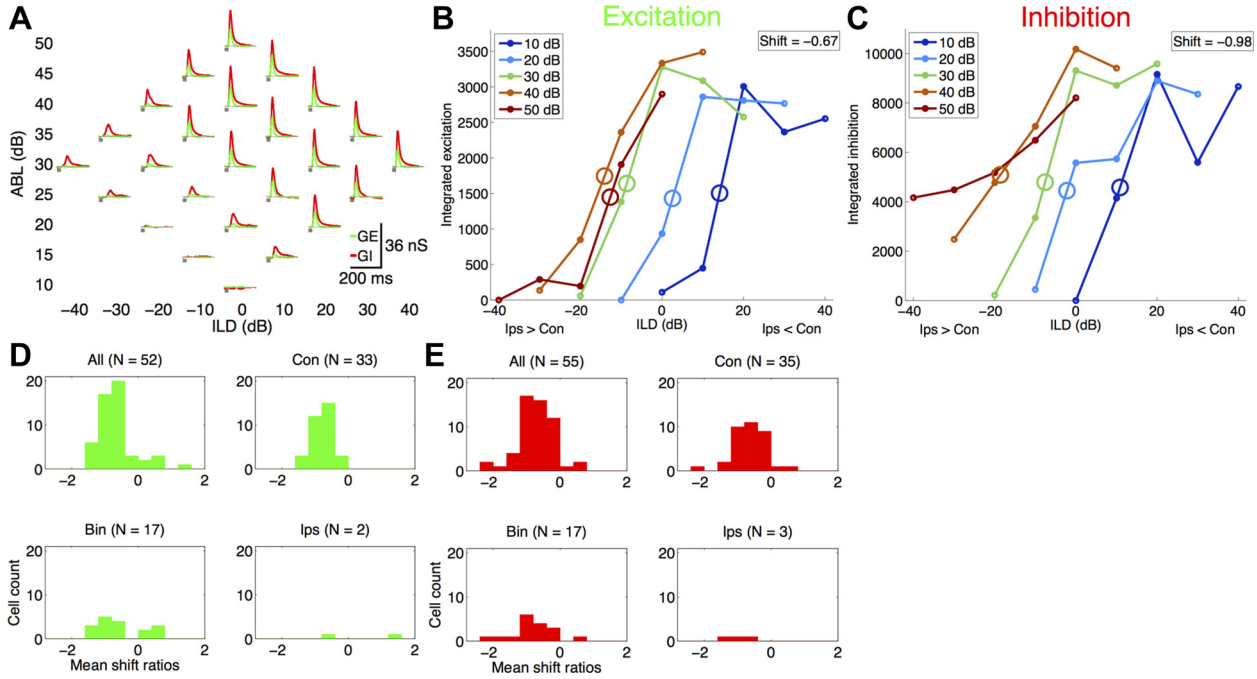

Fig. 3. Synaptic conductance ILD responses in the rat auditory cortex shift toward the ipsilateral ear with increasing ipsilateral sound level. *A*: representative example showing negative ILD response shifts to both excitatory (G_E, green) and inhibitory (G_I, red) conductance responses to the binaural stimulus array (*cell 072810-MK-3-1*). White noise bursts (25-ms duration) are indicated in gray. *B* and *C*: integrated synaptic conductance ILD curves (*B*: excitatory; *C*: inhibitory). Ipsilateral level held constant for each curve as a function of ILD. This cell was contralateral preferring and had a mean ILD response shift of −0.67 dB/dB for excitation (*B*; SD = 0.61) and −0.98 dB/dB for inhibition (*C*; SD = 0.4). *D* and *E*: population histograms showing that the majority of cells (88.5%) had negative G_E response shifts (*D*, *top left*, 46/52 cells) and 94.5% of cells had negative G_I response shifts (*E*, *top left*, 52/55 cells), regardless of binaural preference categorization.

significant (P = 3.4e-98, mean bootstrapped shift: −1.05, SD = 0.11).

In our voltage-clamp whole cell sample, 52/73 cells had robust G_Es and met our inclusion criteria (Fig. 3*D*). Of these cells we found that 46/52 had negative response shifts, with a mean shift of −0.65 dB/dB (SD = 0.58), which was significantly negative at the population level (P = 1.1e-10, 1-sample t-test). Each of the 46/52 negative response shifts was significantly negative (at the $P < 0.05$ level, as tested by bootstrap resampling). We found no significant differences between the response shifts in the contralateral-preferring and binaural-preferring categories (independent samples t-test, P = 0.24). Again, using an arbitrary cutoff of −0.4 dB/dB, we found that 82.7% of our cells had response shifts that were significantly lower than this cutoff value (43/52 cells, P = 0.003, 1-sample t-test).

Additionally, in our voltage-clamp data set, 55/73 cells had robust G_Is and met our inclusion criteria (Fig. 3*E*). Of these cells we found that 52/55 had negative response shifts, with a mean shift of −0.75 dB/dB (SD = 0.53), which was significantly negative at the population level (P = 1.3e-14, 1-sample t-test). Each of the 52/55 negative response shifts was significantly negative (at the $P < 0.05$ level, as tested by bootstrap resampling). We found no significant differences between the response shifts in each binaural preference category (independent samples t-test, all $P > 0.18$). Again, using the arbitrary cutoff of −0.4 dB/dB, we found that 72.7% of our cells had response shifts that were significantly lower than this cutoff value (40/55 cells, P = 1.0e-5, 1-sample t-test).

Finally, we asked whether excitatory or inhibitory synaptic conductances were predictive of firing rate and membrane potential response shifts. Using linear regression we found that excitatory response shifts were not predictive of firing rate (R^2 = 0.64, slope = 1.5, P = 0.4, 3 cells) but did predict membrane potential response shifts (R^2 = 0.22, slope = 0.56, P = 0.013, 27 cells). Inhibitory response shifts did not predict firing rate (R^2 = 0.01, slope = 0.34, P = 0.91, 4 cells) or membrane potential response shifts (R^2 = 0.001, slope = −0.01, P = 0.97, 26 cells). Additionally, at the population level the mean excitatory and inhibitory ILD response shifts were the same (P = 0.588, independent samples t-test) but were uncorrelated with each other (Pearson's ρ = 0.27, P = 0.25, 20 cells).

DISCUSSION

Here we report that ILD sensitivity in rat auditory cortical neurons is strongly dependent upon increasing sound levels. We found that as overall sound levels increased ILD response functions showed significant shifts toward the ipsilateral ear in spiking, membrane potential, and G_E and G_I responses. These shifts occurred regardless of whether the recorded cell responded preferentially to contralateral, ipsilateral, or binaural sounds.

How does the brain accomplish sound localization with invariance to total sound level? In the LSO, neuronal ILD response shifts are strongly level-dependent (Tsai et al. 2010). This means that early in the processing pathway changes in firing rate could indicate changes in sound location, sound level, or both. Tsai and colleagues (2010) suggested that the ICC corrects this ambiguity by comparing the information from the right and left LSOs via a subtraction model that ultimately leads to sound localization performance that is level-independent, as is seen at the perceptual level (Sabin et al. 2005). One possible scenario is that level dependence decreases gradually with each subsequent processing center, from LSO, to ICC, auditory cortex, and ultimately perception. We reasoned that because sound localization performance is level-invariant, there should be a processing center that encodes ILD in a level-invariant way. Stecker and colleagues (2005) hypothesized that the switch from level-dependent to level-independent tuning occurs in a higher cortical area beyond the auditory cortex. Our results support this hypothesis, because we still observed ILD response shifts at the level of the auditory cortex, suggesting that ILD processing is not complete at this point. Another possibility is that although the perception of sound location is level-independent, there need not be an explicit cortical representation of space that is also level-independent. If this were the case, level dependence might be removed when this information is transformed into motor output, for example, in the superior colliculus (Salminen et al. 2012). Yet another possibility is that rats, unlike humans, show level dependence even at the level of behavioral output. This possibility remains to be tested. It is also possible that cortical ILD processing could change with further maturation, experience-dependent plasticity, or other forms of cortical plasticity.

Although we focused here on ILD processing within the rat auditory cortex, whether and how ILD responses are processed beyond the auditory cortex remains poorly understood. Our results indicate that auditory cortical neurons have level-dependent ILD tuning, but whether or how rats end up with level-invariant perception of sound location remains mysterious. To further understand the implications of cortical ILD response shifts, additional studies investigating this property within the ICC, thalamus, and areas beyond the auditory cortex are required. It is also critical to determine whether perceptual sound localization in rats is level-invariant or not. Studies such as these will provide further clarification as to where changes in ILD response shifts occur within the auditory processing pathway, how ILD responses are transformed at each processing level, and ultimately how these transformations define our perception of sound.

Comparison with other studies. Recordings in the LSO of the cat (Tsai et al. 2010) and free-tailed bat (Park et al. 2004) show ILD response curves that shift toward the ipsilateral (excitatory) ear. We found that auditory cortical neurons also showed a shift toward the ipsilateral ear. However, it is important to note that cells in the LSO are almost exclusively driven by the sounds presented to the ipsilateral ear. In the ICC and the auditory cortex, by contrast, most cells are driven by sounds presented to the contralateral ear (because of decussation, in which fibers cross the midline), although many cells are also driven by binaural sounds, especially in SRAF, and in rare cases by ipsilateral sounds. Thus, although neurons in the rat auditory cortex and the cat LSO both show ipsilateral shifts, these shifts are in opposite functional directions (i.e., toward the typically inhibitory and excitatory ears, respectively). In the free-tailed bat, approximately half of the cells in the ICC are invariant to increasing sound levels. The remaining cells have leftward, rightward, or mixed shifts with no net shift at the population level (Park et al. 2004). Park and colleagues

therefore suggested that the ICC might be the origin of ILD invariance observed in human sound localization performance.

Two studies have reported level invariance in the auditory cortex. First, in the pentobarbital-anesthetized pallid bat, increasing sound levels produced a diversity of free-field azimuth responses, with about half of the cells showing invariance (Razak 2011). Interestingly, the other half of their cells were level-dependent but shifted toward the contralateral ear, in the opposite direction from what we observed in the rat. In the second study, in the awake marmoset, free-field sounds from a variety of azimuths and elevations elicited response profiles that were invariant with increasing sound levels (Zhou and Wang 2012). Why do our results in the rat auditory cortex differ from those in the pallid bat and marmoset? One possibility is that level dependence could differ between ILD and free-field stimuli. The invariance observed in these two free-field studies could be the result of integration of ILD cues with ITD and head-related transfer function cues from the cortex or other auditory processing areas, such as the ICC. In other words, it is possible that ILD cues alone could have shown ILD response shifts in these species, but for free-field stimuli the other two binaural cues might have somehow corrected for the shift. This could be tested by directly comparing ILD to free-field responses in the same neurons, for example, with the methods used by Razak (2011) or Campbell et al. (2006b). A related possibility is that ITD cues help produce level invariance of ILD sensitivity, perhaps during development, but that this process is absent in species such as rats that do not use ITD cues for sound localization (Wesolek et al. 2010). In this context it would be interesting to test whether ILD sensitivity is also level-dependent in other species that do not use ITD cues, such as mice. It is also intriguing that rats, unlike the species mentioned above, do not suffer deficits in sound localization following lesions to auditory cortex (Kelly 1980; Kelly and Glazier 1978; Kelly and Kavanagh 1986). Sound localization in rats therefore appears to differ in multiple ways from other species.

Another possible explanation for these species differences is based on the hypothesis that sound localization performance is related to the width of visual acuity, which was proposed by Heffner (2004) (also see Phillips et al. 2012). Heffner surveyed all known sound localization studies in mammals and found a strong correlation between sound localization acuity and the width of the field of best vision (Fig. 10 in Heffner 2004). This makes sense, because high-acuity sound localization is important to accurately orient the fovea for animals that have them, like humans, but is less important for animals such as rats that have a broad field of best vision instead of a fovea. Thus the sound localization errors due to level dependence would be very costly for cats, bats, and marmosets, which all have narrow visual fields, and therefore would likely provide strong evolutionary pressure toward level invariance of sound localization. Because of their broad field of best vision, sound localization errors are much less costly for rats, and they may be able to tolerate the errors due to level dependence. This account predicts that perceptual sound localization performance should be level-dependent in rats, which remains to be tested.

Another possible reason for the difference between our findings and other work in the auditory cortex could arise from anesthesia. However, this seems unlikely since studies in both the awake bat (Park et al. 2004) and ketamine-anesthetized cat (Tsai et al. 2010) show strong evidence of ILD level dependence in the LSO. Additionally, invariance was observed in the awake cat (Mickey and Middlebrooks 2003) and marmoset (Zhou and Wang 2012) as well as in the pentobarbital-anesthetized pallid bat (Razak 2011). Thus anesthesia seems unlikely to be the reason for the differences between our study and others.

In the auditory cortex, a large proportion of cells are contralateral preferring, especially in A1 (Chadderton et al. 2009; Imig and Adrian 1977; Kelly and Sally 1988; Phillips and Irvine 1983; Zhang et al. 2004; but see Campbell et al. 2006a). However, a higher proportion of cells in the SRAF of auditory cortex are binaural preferring (Higgins et al. 2010). We wondered whether all cells, and not just contralateral-preferring cells, in the auditory cortex were level-invariant to ILD stimuli. We therefore did not restrict our recordings to A1. On the basis of our coarse mapping of the auditory cortex using extracellular recordings, ~80% of our cells were located in either A1 or SRAF, with the remaining cells located in either VAF or PAF. To our surprise, nearly all of the neurons in our sample had significant ILD shifts toward the ipsilateral ear, throughout these cortical regions. When we subdivided our recordings into specific auditory fields we found no significant differences between the ILD response shifts in these fields.

Cortical inhibition does not appear to shape ILD response shifts. The negative ILD response shifts we observed in the rat auditory cortex did not appear to be shaped by local cortical inhibition. If synaptic processing within the rat auditory cortex had a role in this computation, then we would have expected to find G_I ILD response shifts that were more positive than the excitatory ILD response shifts. In that case, active inhibitory shaping would have caused spiking and membrane potential ILD response functions to have more negative shifts than those we observed in the G_E ILD response shifts. Instead, we observed highly significant negative response shifts in all response types, with no significant differences between spiking, membrane potential, and conductances at the population level. We found that excitatory ILD response shifts significantly predicted membrane potential ILD shifts. However, G_E and G_I response shifts were uncorrelated, and inhibitory response shifts did not predict membrane potential response shifts. Thus our results are consistent with inheritance from presynaptic inputs, since the spiking and membrane potential ILD response shifts matched those of excitatory synaptic inputs. Why, then, are the response shifts of inhibitory inputs uncorrelated with excitation? One possible explanation is that inhibition is involved with a different form of ILD processing, such as the shaping of binaural preferences of cortical cells (Razak and Fuzessery 2010). With our whole cell approach, we should be able to test for this possibility.

ACKNOWLEDGMENTS

We thank Aldis Weible and Alexandra Moore for thoughtful discussions and the University of Oregon Animal Care Services for taking exceptional care of our lab animals.

GRANTS

This work was supported by the National Institutes of Health, the Post-9/11 Montgomery GI bill, and the Whitehall Foundation.

DISCLOSURES

No conflicts of interest, financial or otherwise, are declared by the author(s).

AUTHOR CONTRIBUTIONS

Author contributions: M.K. and M.W. conception and design of research; M.K. and W.S. performed experiments; M.K. analyzed data; M.K., W.S., and M.W. interpreted results of experiments; M.K. prepared figures; M.K. and W.S. drafted manuscript; M.K. and M.W. edited and revised manuscript; M.K. and M.W. approved final version of manuscript.

REFERENCES

Altshuler MW, Comalli PE. Effect of stimulus intensity and frequency on median horizontal plane sound localization. *J Aud Res* 15: 262–265, 1975.

Barry PH. JPCalc, a software package for calculating liquid junction potential corrections in patch-clamp, intracellular, epithelial and bilayer measurements and for correcting junction potential measurements. *J Neurosci Methods* 51: 107–116, 1994.

Campbell RA, Schnupp JW, Shial A, King AJ. Binaural-level functions in ferret auditory cortex: evidence for a continuous distribution of response properties. *J Neurophysiol* 95: 3742–3755, 2006a.

Campbell RA, Doubell TP, Nodal FR, Schnupp JWH, King AJ. Interaural timing cues do not contribute to the map of space in the ferret superior colliculus: a virtual acoustic space study. *J Neurophysiol* 95: 242–254, 2006b.

Chadderton P, Agapiou JP, McAlpine D, Margrie TW. The synaptic representation of sound source location in auditory cortex. *J Neurosci* 29: 14127–14135, 2009.

Chang EF, Bao SW, Imaizumi K, Schreiner CE, Merzenich MM. Development of spectral and temporal response selectivity in the auditory cortex. *Proc Natl Acad Sci USA* 102: 16460–16465, 2005.

de Villers-Sidani E, Chang EF, Bao SW, Merzenich MM. Critical period window for spectral tuning defined in the primary auditory cortex (A1) in the rat. *J Neurosci* 27: 180–189, 2007.

DeWeese MR, Wehr M, Zador AM. Binary spiking in auditory cortex. *J Neurosci* 23: 7940–7949, 2003.

Grothe B, Pecka M, McAlpine D. Mechanisms of sound localization in mammals. *Physiol Rev* 90: 983–1012, 2010.

Heffner HE, Heffner RS, Contos C, Ott T. Audiogram of the hooded Norway rat. *Hear Res* 73: 244–247, 1994.

Heffner RS. Primate hearing from a mammalian perspective. *Anat Rec A Discov Mol Cell Evol Biol* 281: 1111–1122, 2004.

Higgins NC, Storace DA, Escabi MA, Read HL. Specialization of binaural responses in ventral auditory cortices. *J Neurosci* 30: 14522–14532, 2010.

Hromadka T, DeWeese MR, Zador AM. Sparse representation of sounds in the unanesthetized auditory cortex. *PLoS Biol* 6: e16, 2008.

Imig TJ, Adrian HO. Binaural columns in the primary field (A1) of cat auditory cortex. *Brain Res* 138: 241–257, 1977.

Irvine DR, Gago G. Binaural interaction in high-frequency neurons in inferior colliculus of the cat: effects of variations in sound pressure level on sensitivity to interaural intensity differences. *J Neurophysiol* 63: 570–591, 1990.

Kapfer C, Seidl AH, Schweizer H, Grothe B. Experience-dependent refinement of inhibitory inputs to auditory coincidence-detector neurons. *Nat Neurosci* 5: 247–253, 2002.

Kavanagh GL, Kelly JB. Midline and lateral field sound localization in the ferret (*Mustela putorius*): contribution of the superior olivary complex. *J Neurophysiol* 67: 1643–1658, 1992.

Kelly JB. Effects of auditory cortical lesions on sound localization by the rat. *J Neurophysiol* 44: 1161–1174, 1980.

Kelly JB, Glazier SJ. Auditory cortex lesions and discrimination of spatial location by the rat. *Brain Res* 145: 315–321, 1978.

Kelly JB, Judge PW, Fraser IH. Development of the auditory orientation response in the albino rat (*Rattus norvegicus*). *J Comp Psychol* 101: 60–66, 1987.

Kelly JB, Kavanagh GL. Effects of auditory cortical lesions on pure-tone sound localization by the albino rat. *Behav Neurosci* 100: 569–575, 1986.

Kelly JB, Masterton B. Auditory sensitivity of the albino rat. *J Comp Physiol Psychol* 91: 930–936, 1977.

Kelly JB, Sally SL. Organization of auditory cortex in the albino rat: binaural response properties. *J Neurophysiol* 59: 1756–1769, 1988.

Koka K, Read HL, Tollin DJ. The acoustical cues to sound location in the rat: measurements of directional transfer functions. *J Acoust Soc Am* 123: 4297–4309, 2008.

Lu JP, Cui YL, Cai R, Mao YT, Zhang JP, Sun XD. Early auditory deprivation alters expression of NMDA receptor subunit NRI mRNA in the rat auditory cortex. *J Neurosci Res* 86: 1290–1296, 2008.

Mickey BJ, Middlebrooks JC. Representation of auditory space by cortical neurons in awake cats. *J Neurosci* 23: 8649–8663, 2003.

Moore MJ, Caspary DM. Strychnine blocks binaural inhibition in lateral superior olivary neurons. *J Neurosci* 3: 237–242, 1983.

Park TJ, Klug A, Holinstat M, Grothe B. Interaural level difference processing in the lateral superior olive and the inferior colliculus. *J Neurophysiol* 92: 289–301, 2004.

Phillips DP, Irvine DR. Some features of binaural input to single neurons in physiologically defined area AI of cat cerebral cortex. *J Neurophysiol* 49: 383–395, 1983.

Phillips DP, Quinlan CK, Dingle RN. Stability of central binaural sound localization mechanisms in mammals, and the Heffner hypothesis. *Neurosci Biobehav Rev* 36: 889–900, 2012.

Pollak GD, Wenstrup JJ, Fuzessey ZM. Auditory processing in the moustache bat's inferior colliculus. *Trends Neurosci* 9: 556–561, 1986.

Polley DB, Read HL, Storace DA, Merzenich MM. Multiparametric auditory receptive field organization across five cortical fields in the albino rat. *J Neurophysiol* 97: 3621–3638, 2007.

Popescu MV, Polley DB. Monaural deprivation disrupts development of binaural selectivity in auditory midbrain and cortex. *Neuron* 65: 718–731, 2010.

Razak KA. Systematic representation of sound locations in the primary auditory cortex. *J Neurosci* 31: 13848–13859, 2011.

Razak KA, Fuzessery ZM. GABA shapes a systematic map of binaural sensitivity in the auditory cortex. *J Neurophysiol* 104: 517–528, 2010.

Recanzone GH, Beckerman NS. Effects of intensity and location on sound location discrimination in macaque monkeys. *Hear Res* 198: 116–124, 2004.

Sabin AT, Macpherson EA, Middlebrooks JC. Human sound localization at near-threshold levels. *Hear Res* 199: 124–134, 2005.

Salminen NH, Tiitinen H, May PJ. Auditory spatial processing in the human cortex. *Neuroscientist* 18: 602–612, 2012.

Scholl B, Gao X, Wehr M. Nonoverlapping sets of synapses drive on responses and off responses in auditory cortex. *Neuron* 65: 412–421, 2010.

Semple MN, Kitzes LM. Binaural processing of sound pressure level in the inferior colliculus. *J Neurophysiol* 57: 1130–1147, 1987.

Stecker GC, Harrington IA, Middlebrooks JC. Location coding by opponent neural populations in the auditory cortex. *PLoS Biol* 3: e78, 2005.

Sykova E. The extracellular space in the CNS: its regulation, volume and geometry in normal and pathological neuronal function. *Neuroscientist* 3: 28–41, 1997.

Tsai JJ, Koka K, Tollin DJ. Varying overall sound intensity to the two ears impacts interaural level difference discrimination thresholds by single neurons in the lateral superior olive. *J Neurophysiol* 103: 875–886, 2010.

Wehr M, Zador AM. Balanced inhibition underlies tuning and sharpens spike timing in auditory cortex. *Nature* 426: 442–446, 2003.

Wesolek CM, Koay G, Heffner RS, Heffner HE. Laboratory rats (*Rattus norvegicus*) do not use binaural phase differences to localize sound. *Hear Res* 265: 54–62, 2010.

Xu F, Cai R, Xu JH, Zhang JP, Sun XD. Early music exposure modifies GluR2 protein expression in rat auditory cortex and anterior cingulate cortex. *Neurosci Lett* 420: 179–183, 2007.

Xu JH, Yu LP, Cai R, Zhang JP, Sun XD. Early continuous white noise exposure alters auditory spatial sensitivity and expression of GAD65 and $GABA_A$ receptor subunits in rat auditory cortex. *Cereb Cortex* 20: 804–812, 2010.

Zhang J, Nakamoto KT, Kitzes LM. Binaural interaction revisited in the cat primary auditory cortex. *J Neurophysiol* 91: 101–117, 2004.

Zhou Y, Wang X. Level dependence of spatial processing in the primate auditory cortex. *J Neurophysiol* 108: 810–826, 2012.